SEMARAK ILMU PUBLISHING

CFD Letters

Journal homepage:
https://semarakilmu.com.my/journals/index.php/CFD_Letters/index
ISSN: 2180-1363

CFD Simulation Analysis of Non-Premixed Combustion using a Novel Axial-Radial Combined Swirler for Emission Reduction Enhancement

Nor Afzanizam Samiran[1,2,*], Khalil Firdaus Abu Mansor[1], Razlin Abd Rashid[1,2], Muhammad Suhail Sahul Hamid[3]

[1] Department of Mechanical Engineering Technology, Faculty of Engineering Technology, Universiti Tun Hussein Onn Malaysia, Pagoh Johor, 84600 Malaysia
[2] Integrated Engineering Simulation and Design (IESD) Focus Group, Universiti Tun Hussein Onn Malaysia, Pagoh Higher Education Hub, 84600 Pagoh, Muar, Johor, Malaysia
[3] Els Energy and Lab Solutions Sdn Bhd No.11A Tingkat Merpati Dua, Taman Transkrian 14300 Nibong Tebal, Pulau Pinang, Malaysia

ARTICLE INFO

Article history:
Received 29 November 2022
Received in revised form 28 December 2022
Accepted 25 January 2023
Available online 1 June 2023

Keywords:
Axial swirler; Emissions; Non-Premixed Combustion; Radial swirler; Temperature; Velocity

ABSTRACT

Combustion industries for many decades dealing with the issues in reducing the emissions without affecting the performance of combustion. The present study aims to investigate the performance of swirler mechanism which combining between both axial and radial types to reduce emissions and increase the mixing process via the non-premixed method. Each of axial and radial swirler consisted with 8 blades vane. Swirl angle for radial swirler is 35° and inclination angle for axial swirler is 15°. The swirler is designed using Solidworks software package and CFD analysis was then performed using ANSYS Fluent software package. The fuel used is liquefied petroleum gas (LPG) gas which contained 30% propane and 70% butane. The turbulence model standard k-epsilon was used in this study. The result found that the combined swirler was capable to reduce CO emission as the complete reaction into CO_2 component was higher. This is due to the broader region of temperature and higher velocity magnitude produced by the combined swirler. However, the maximum temperature result for axial swirler was higher than the combined swirler. As a recommendation, the inclination blade angle in the axial swirler of the combined swirler should be increased to increase the temperature value.

1. Introduction

Global environmental problems due to emissions from combustion such as greenhouse warming, acid rain, and the hole in the ozone layer have become serious problems all over the world. Greenhouse warming is a global problem and difficult to solve as acid rain is essentially a regional phenomenon. For a gas turbine (GT) sector, optimal efficiency and optimum output are vital in order to reduce pollutant emissions in accordance with current legislation [1]. Advanced design in combustion systems such as using the swirler mechanism was one of the potential solutions to reduce emissions [2].

* *Corresponding author.*
E-mail address: afzanizam@uthm.edu.my (Nor Afzanizam Samiran)

https://doi.org/10.37934/cfdl.15.6.111

Studies in swirl flows were conducted for many decades due to their extensive application in various types of practical systems, including gas turbine combustion. Frequent experiments in swirl fluxes have been carried out from fundamental isothermal and reacting flows to those formed in critical swirl combustor geometries. Experimental results typically produced general characteristics of swirl flows and revealed important effects of swirl on the promotion of flame stability, improved combustion efficiency, and regulation of controlling the emission of pollutants from combustion.

The geometrical development technique of flame stabilization in industrial plants is based on increasing the reactive gas residence time, either through the bluff body enhancement effect or the rotating flow via the swirling mechanisms or by a combination of these two elements. The swirl burner is a common name for helical flow burners which is attributed to very wide industrial applications. Other studies focused on the effects of hurling, stabilization, blowout, and pollutant emissions on the characteristics of lifted flames [3].

Swirling flow burners have been important for both premixed and non-premixed combustion systems due to their beneficial effects on flame stability, combustion intensity, and combustion performance. One of the critical issues with the design of gas turbine engine is how emissions like carbon dioxide and carbon monoxide are minimized. Gas turbine manufacturers typically used lean premixed combustion techniques to achieve low NOx emissions. However, although the usage of lean pre-premixed combustion is attractive to reduce pollution, it requires a complicated system, increases the size and weight of the system, and produces acoustic instability.

Swirling can be used in non-premixed combustion nowadays, and in particular nitrogen oxide emissions can be decreased. The inflammation temperature decreases under the swirl effect and hence improved the mixing process of reactants thus reduce the production of NOx. Moreover, the increase in the swirl number causes a reduction of the residence time in heat areas if the intensity of the swirl is sufficient. This also reduces the formation of NOx. However, a swirling intensity needs to be identified as to achieve both a compromise between reducing pollutant emissions and preventing the flame-burning distance [3].

Study on swirl combustion using CFD simulation analysis has been previously investigated by few researchers. Hu *et al.,* [4] examined effects of swirlers with blade angles and applied voltage of plasma actuators on combustion and wall temperature of a Can - type gas turbine combustor. Results show that CO emission decreases with the increase of the blade angle. The reduction of CO emission were 67.6%, 95.9% and 99.6% with the blade angles of 45◦, 50◦ and 55◦ respectively compared to the maximum value of CO emission for a 40◦ blade angle. Jing *et al.,* [5] presents a computational fluid dynamic investigation on the burning features of a methanol swirling combustor with two stages of swirling blades (45°+45°, 60°+60°, and 45°+60°). The results show that the blade angle design of 45°+ 60° displays high potential of combustion characteristics at which the NOx and CO emissions are measured to be 27.0 and 11.0 mg/m^3. Hosseini *et al.,* [6] study the effect of inlet air swirl number of a Methane-Air Diffusion Flame on dynamic stream characteristic, temperature, and radiation heat flux distribution via the analysis of ANSYS Fluent CFD code. The results showed that increases in swirl number increase the flux radiation efficiency by 36.5% and reduces the pollutant NOx by 58.6%. Matthujak *et al.,* [7] studied a swirling flow in domestic LPG burners with inclined and swirl angle of 50◦ and 15◦ respectively and its characteristics on thermal efficiency augmentation. The results reporterd that swirling flow does increase the maximum combustion temperature and the net heat flux into the vessel, directly enhancing the heat conversion efficiency and thus increasing the thermal efficiency. Pashchenko [8] conducted the CFD-modeling of synthetic (hydrogen-rich) fuel combustion in a swirling flame. The results showed that NOx emission was increased from 88.9 ppm to 93.1 ppm for synfuel with increased of hydrogen mole fraction from 0.4 to 0.8.

The present study is critical in the area of burning systems with low-emission and high energy-efficient of swirl burner technologies, as the fundamental knowledge of the swirl effect on combustor efficiency is still minimal. Previous study typically focused on the analysis of swirl angle and number of swirler's blade for conventional either axial or radial swirler. However, a specific study which combined both axial and radial swirler seems rarely investigated. Thus, the present study aims to assess the effect of a novel concept of combined axial-radial swirl mechanism flow on the burner performance. The characteristic of thermal efficiency, carbon monoxide (CO) and carbon dioxide (CO_2) emission characteristics were examined. The results obtained in this work provide a fundamental understanding on the parameters that is dominant in thermal efficiency and emissions pollution. Besides, the findings are considerable significance in providing design or working mechanisms and real applications for the manufacturing of the swirl burner that usually used in the industries of petroleum gas and gas turbine combustion.

2. Method

2.1 Swirl Geometry Development

The design of swirler was developed using Solidworks software package. The novel design involved a combination of both axial and radial swirler as shown in Figure 1 (a) and (b). The swirler is consist of outer swirler of radial type at the first stage followed by inner swirler of axial type at the second stage.

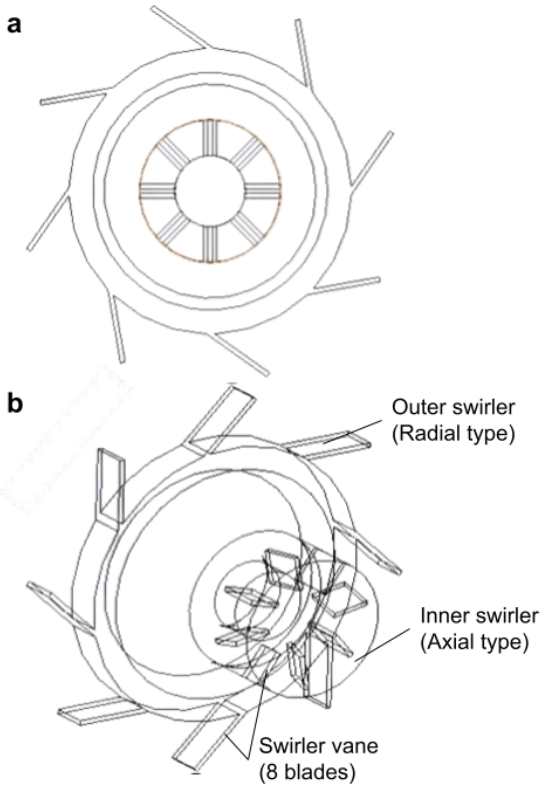

Fig. 1. Axial-radial combined swirler (a) top view (b) isometric view

The diameter for the outer and inner section of the radial and axial swirler is 120 mm and 60 mm respectively. The fuel inlet is 30 mm. Radial and axial swirler were consisted of 8 blades. Inclination angle for axial swirler vane is 15^o and radial vane angle is 35^o. A conventional axial swirler was used

as a baseline in this study. The air and fuel inlet were set to 60mm and 30mm respectively. Figure 2 (a) and (b) showed the conventional axial swirler model as a baseline study. The inclination angle of the conventional axial swirler vane was also set to 15 degrees and contained 8 swirl blades.

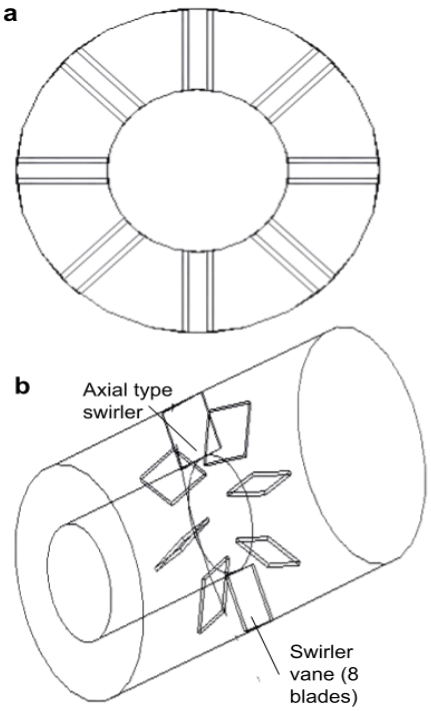

Fig. 2. Conventional axial swirler (a) top view (b) isometric view

2.2 Governing Equations

The molecular structure of fluids does not demonstrate resistance to external shear forces. Every single action, therefore, creates a motion for fluid substances. By continuum assumption, all fluids shall abide by the laws of motion. According to the Ferziger [9], conservation of mass, momentum and scalars (energy, species, etc.) should therefore be maintained for control volume. Conservation equations for Cartesian coordinates can be written as follows:

For conservation of mass:

$$\frac{\partial \rho}{\partial t} + \frac{\partial (\rho u_1)}{\partial x_i} = \frac{\partial \rho}{\partial t} + \frac{\partial (\rho u_x)}{\partial x} + \frac{\partial (p u_y)}{\partial y} + \frac{\partial (\rho u_z)}{\partial z} = 0 \quad (1)$$

For conservation of momentum:

$$\frac{\partial (p u_i)}{\partial t} + \frac{\partial (\rho u_j u_j)}{\partial x_j} = \frac{\partial \tau_{jj}}{\partial x_j} - \frac{\partial p}{\partial x_1} + \rho g_i \quad (2)$$

For conservation of scalars:

$$\frac{\partial (\rho \phi)}{\partial t} + \frac{\partial (\rho u_j \phi)}{\partial x_j} = \frac{\partial}{\partial x_j}\left(\Gamma \frac{\partial \phi}{\partial x_j}\right) + q_\phi \quad (3)$$

2.3 Turbulence Model

Introduced the k-ε model. The idea of the model is to explain the turbulent viscosity of the turbulence equations of development and destruction. Empirical relationships are constructed using experimental data. For the k-ε model, turbulent viscosity is described as:

$$\mu_t = \bar{\rho} C_\mu \frac{k^2}{\varepsilon} \tag{4}$$

where ε dissipates turbulent kinetic energy, k and ε are represented by the closure of two equations of balance:

$$\frac{\partial}{\partial t}(\bar{\rho}k) + \frac{\partial}{\partial x_i}(\bar{\rho}\tilde{u}_i k) = \frac{\partial}{\partial x_i}\left[\left(\mu + \frac{\mu_t}{\sigma_k}\right)\frac{\partial k}{\partial x_i}\right] + P_k - \bar{\rho}\varepsilon \tag{5}$$

$$\frac{\partial}{\partial t}(\bar{\rho}\varepsilon) + \frac{\partial}{\partial x_i}(\bar{\rho}\tilde{u}_i \varepsilon) = \frac{\partial}{\partial x_i}\left[\left(\mu + \frac{\mu_t}{\sigma_\varepsilon}\right)\frac{\partial \varepsilon}{\partial x_i}\right] + C_{\varepsilon 1}\frac{\varepsilon}{k}P_k - C_{\varepsilon 2}\bar{\rho}\frac{\varepsilon^2}{k} \tag{6}$$

The source term P_k is given by:

$$P_k = -\bar{\rho}\mathrm{u}_\mathrm{i}^{\pi}\mathrm{u}_\mathrm{j}^{\prime\prime}\frac{\partial \tilde{u}_i}{\partial x_j} \tag{7}$$

Table 1 shows the standard model constants. As these consistencies are derived from experimental results, the k/μ model for the wide range of wall bounded and free shear flow forms is comparably precise. However, other types of flows, including swirling flows, may have to be improved.

Table 1
Constant values used in standard k–ε turbulence model

$C_{\varepsilon 1}$	1.44
$C_{\varepsilon 2}$	1.92
C_μ	0.09
σ_k	1.0

2.4 Grid Development

Meshing was developed to coordinate the boundary condition calculation region of air inlet, fuel inlet, outer wall and outlet as shown in Figure 3. The combine swirler design attributed 8 air inlets which relative to the 8 blades of radial swirler. The growth rate of mesh was set to 1.2. The generated mesh of the model produced 68900 elements with average orthogonal mesh quality of 0.97653. The aforementioned orthogonal quality value is considered as an excellent quality of generated mesh which typically ranged between 0.9 to 1 [10]. The maximum size, defeature, minimum curvature, normal angle curvature size was set to 9.841e^{-2} m, 2.460e^{-4}m, 0.003m and 18^o respectively. Average surface area and minimum edge length were set to 1.2328e^{-2} m^2 and 0.03m respectively.

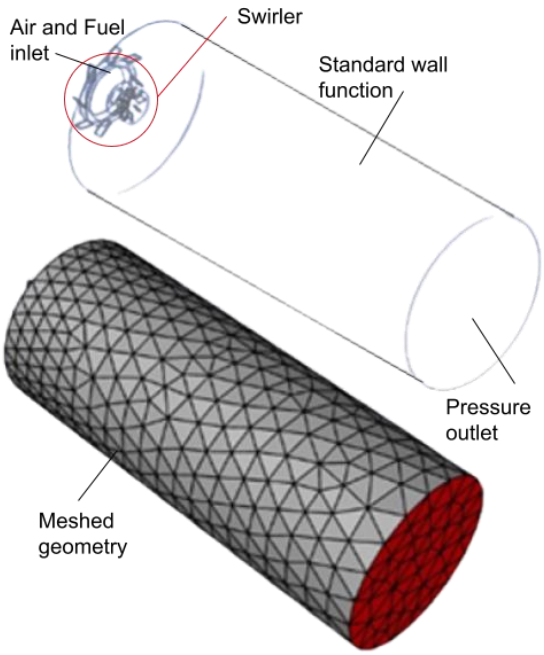

Fig. 3. Boundary condition and meshed geometry

2.5 Boundary Condition and Solver Setup

The dimension of combustor length and diameter were 800 mm and 320 mm respectively. The length and diameter of combustor was determined based on the typical dimension of industrial combustion chamber which ranged between 700 mm to 1000 mm and 200 mm to 400 mm respectively [11-14]. The type of fuel used was liquefied petroleum gas (LPG) which consisted of propane and butane with mixing ratio of 0.3 and 0.7 [15]. The properties of LPG were set based on the Table 2. The boundary condition involved a region of air-fuel inlet and pressure outlet. The air and fuel flowrate at air and fuel inlet were set to 0.1kg/s and 0.003kg/s respectively. The temperature of air and fuel were set to 350K and 300K respectively. The air and fuel flowrate and temperature were set based on typical setup for LPG combustion via CFD simulation analysis [13, 15, 16]. Pressure in combustor was set to 2 atm. Standard wall function has been used for near wall treatment. Standard k-e turbulent model was used to model the flow.

Table 2
Physical properties of propane and butane [17]

Property	Propane	Butane
Liquid density, kg/m^3	509	585
Calorific value, MJ/kg	46.34	45.56
Boiling point, ^{o}C	-42	-0.5

The solution method parameter setup was using SIMPLE scheme for pressure velocity coupling and least square cell based for gradient characteristic. Pressure, momentum and energy were using second order upwind scheme. Whereas turbulent kinetic energy and turbulent dissipation rate were using first order upwind scheme.

Figure 4 showed the validation results of the present CFD simulation model with the results from the previous experimental work which also used axial swirl combustion technique and LPG as a fuel. Previous work was typically used combustion chamber with diameter less than 0.2 m for LPG

combustion. Hence, the present study intends to investigate the combustion characteristic at the region above 0.2 m of combustor length. At the region ranged from 0 to 0.2 m, the present results were typically within the range between the results of Xinzhuo and Vipul & Rupesh. The deviation of error seems due to other actual factor associated with the experimental condition which was not appropriately modelled using simulation method such as, wall insulation effect, environmental humidity, different fuel fraction and etc. However, the present result considered in good agreement as the percentage error was less than 20%. Thus, the present CFD model was acceptable to be used for simulation model in this study.

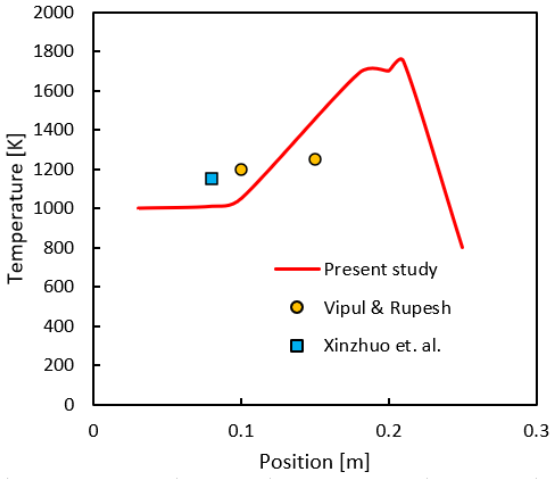

Fig. 4. Validation result with previous experimental work [18, 19]

3. Result and Discussion

The present study compares the combustion performance between a radial-axial combined swirler with the conventional axial swirler. The CFD analysis using ANSYS software package was performed to investigate the effectiveness of the combined swirler in reducing the emission and improving the gradient of velocity and temperature. Figure 5 (a) and Figure 6 (a) shows the contour of velocity magnitude for the combined swirler and conventional axial swirler. The distribution of velocity magnitude flow was smaller for combined swirler compared to conventional axial swirler. However, the maximum value of velocity magnitude for combined swirler was higher than conventional axial swirler. The results were also clearly illustrated as in Figure 7 (a).

Figure 5 (b) and Figure 6 (b) showed the temperature distribution between combined swirler and conventional axial swirler. The higher temperature region for conventional axial swirler seems to axially propagated from burner nozzle to combustor outlet. Whereas combined swirler produced wider region of higher temperature in the combustor chamber. Although the higher temperature region is wider, the maximum value of temperature for combined swirler was lower compared to conventional axial swirler. Lower temperature value is a good indication for lower production of NOx emission.

Whereas wider distribution of higher temperature is good indication of complete combustion reaction throughout the chamber to produce CO_2 hence reduce the incomplete reaction of CO emission. Thus, combined swirler seems to attributed good characteristic of emission reduction compared to conventional axial swirler.

Figure 5 (c) and Figure 6 (c) showed the mass fraction of CO_2 distribution between combined swirler and conventional axial swirler. The distribution of CO_2 mass fraction was correlated with the

distribution of temperature. This indicate that higher region of temperature promoted higher complete reaction region of CO_2. Figure 5 (d) and Figure 6 (d) showed the distribution of CO mass fraction produced using combined swirler and conventional axial swirler. The distribution penetration of CO mass fraction using conventional axial swirler was broader compared to combined swirler. Conventional axial swirler seems to produced higher mass fraction of unreacted CO element. Hence this indicate that combined swirler exhibited good mixing characteristic in terms of complete reaction compared to axial swirler.

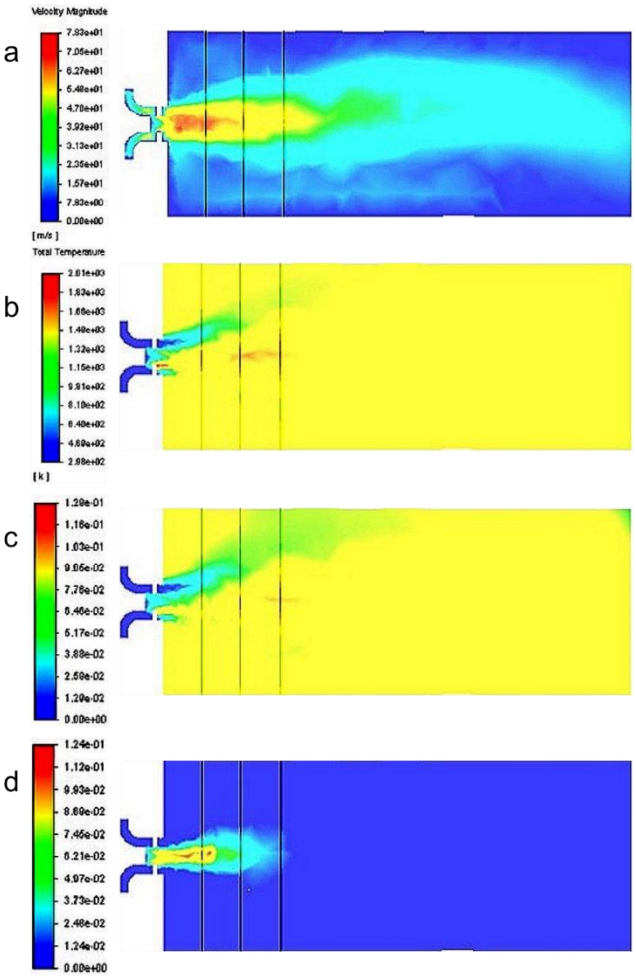

Fig. 5. Contour results of axial-radial combined swirler for (a) velocity magnitude (b) Temperature (c) CO_2 mass fraction (d) CO mass fraction

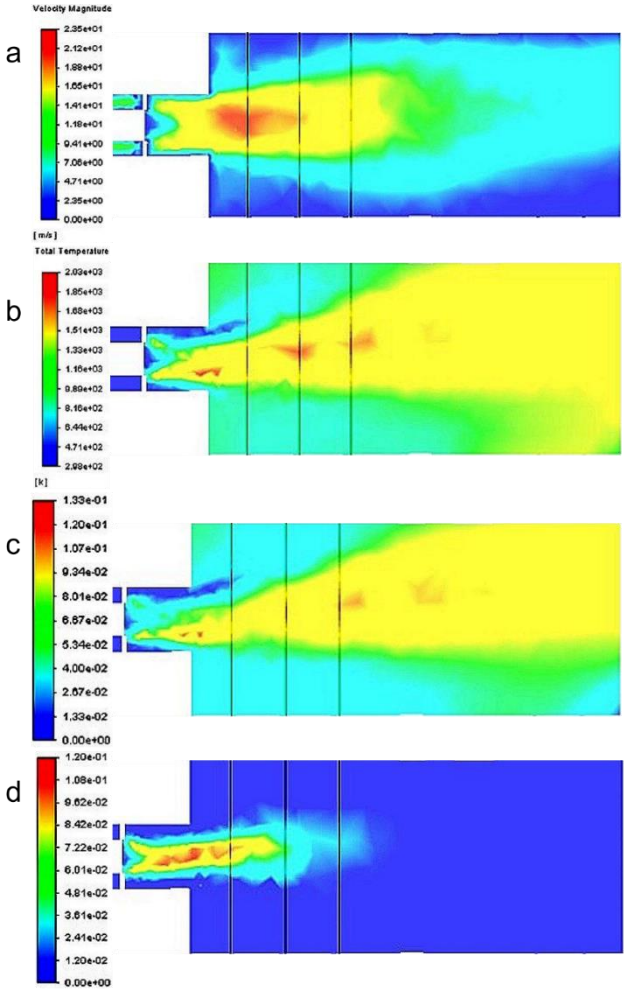

Fig. 6. Contour results of conventional axial swirler for (a) velocity magnitude (b) Temperature (c) CO_2 mass fraction (d) CO mass fraction

Figure 7 (a) shows the velocity magnitude for combined swirler and axial swirler at 0.065m from the burner nozzle. The result showed that combined swirler exhibited higher maximum velocity magnitude typically at the radial position between 0.1 to 0.3 m compared to axial swirler. The higher velocity magnitude promoted the higher mixing rate as well as reduced the blowoff tendencies [20]. Those aforementioned characteristics increase the probability of complete reaction to occur. Figure 7 (b) shows the temperature distribution between combined swirler and axial swirler. The conventional axial swirler produced higher maximum temperature (1724 K) compared to combined swirler (1650 K). However combined swirler produced higher temperature at the most region radially which were between 0 to 0.5 m and 0.25 to 0.4 m. This indicate that the distribution of higher temperature was more homogenous using combined swirler hence promoted wider region of

complete combustion. Figure 7 (c) showed the distribution of CO_2 mass fraction between combined swirler and axial swirler. The results were correlated with the distribution temperature results. The region with higher temperature caused the complete reaction into CO_2 and H_2O to occur. Hence combined swirler produced higher CO_2 mass fraction than axial swirler at most of the radial region. This indicate that combined swirler seems to exhibited better mixing air-fuel characteristic for complete reaction to take place. Figure 7 (d) showed that combined swirler produced lower distribution of CO mass fraction than axial swirler. This result also is in good agreement or correlated with the distribution of temperature and CO_2 mass fraction. A combined swirler produced more homogenous mixing with higher temperature hence the complete reaction to CO_2 is higher than the axial swirler, thus reducing the amount of unreacted CO species. This is a good indication that combined swirler can potentially reduce the emission of CO at the combustor exit.

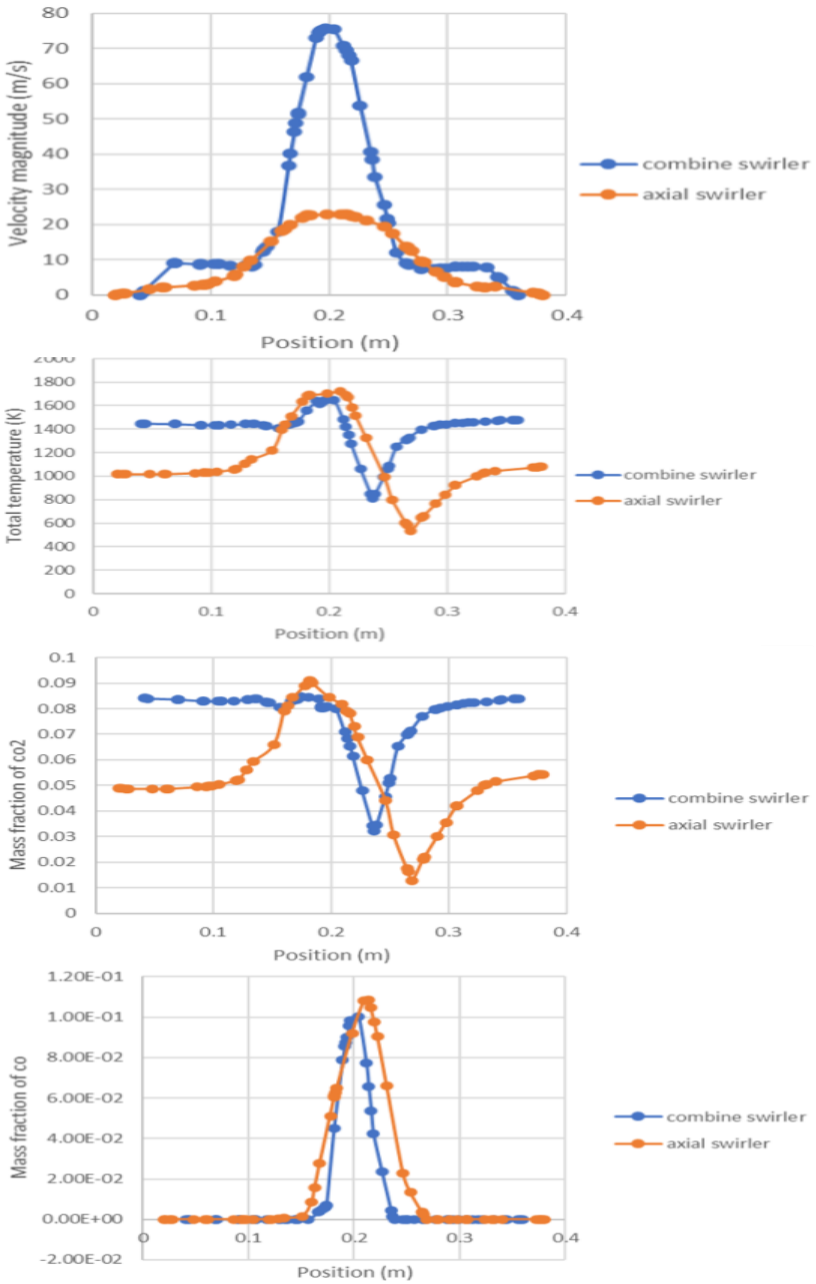

Fig. 7. Performance comparison between axial-radial combined swirler and conventional axial swirler for (a) velocity magnitude (b) Temperature (c) CO_2 mass fraction (d) CO mass fraction

4. Conclusion

The present study aims to investigate the performance of a novel axial-radial combination swirler design in reducing the combustion emission and increasing the rate of complete reaction. The combustion characteristic of conventional axial swirler was also investigated as a baseline. The study was conducted using CFD simulation method. The results showed that combined swirler exhibited higher velocity magnitude distribution than axial swirler. Higher velocity magnitude indicates higher mixing rate and lower blowoff tendencies. Thus, combined swirler seems to exhibited good combustion characteristic. The combined swirler also produce broader region of higher temperature as well as complete reaction of CO_2 mass fraction value compared to axial swirler. This indicate that combined swirler demonstrate higher tendencies of complete reaction than axial swirler. The production of CO was also lower using combined swirler compared to axial swirler. Thus, a new design of combined swirler is highly potential to be use to reduce emission and increase the combustion efficiency.

Acknowledgement
This research was supported by Ministry of Higher Education (MOHE) through Fundamental Research Grant Scheme (FRGS) (FRGS/1/2019/TK07/UTHM/03/2) and Universiti Tun Hussein Onn Malaysia (UTHM) through Tier 1 (vot Q030)

References

[1] Subash, Arman Ahamed, Senbin Yu, Xin Liu, Michael Bertsch, Robert-Zoltan Szasz, Zhongshan Li, Xue-Song Bai, Marcus Aldén, and Daniel Lörstad. "Flame investigations of a laboratory-scale CECOST swirl burner at atmospheric pressure conditions." *Fuel* 279 (2020): 118421. https://doi.org/10.1016/j.fuel.2020.118421

[2] Hasan, Karrar S., Wisam A. Abd Al-wahid, and H. H. S. Khwayyir. "Flashback and combustion stability in swirl burners." In *IOP Conference Series: Materials Science and Engineering*, vol. 928, no. 2, p. 022045. IOP Publishing, 2020. https://doi.org/10.1088/1757-899X/928/2/022045

[3] Mansouri, Zakaria, and Toufik Boushaki. "Investigation of large-scale structures of annular swirling jet in a non-premixed burner using delayed detached eddy simulation." *International Journal of Heat and Fluid Flow* 77 (2019): 217-231. https://doi.org/10.1016/j.ijheatfluidflow.2019.04.007

[4] Hu, Zhenwei, Jie Sun, Jin Wang, Ting Ma, Jakov Baleta, and Bengt Sundén. "Effects of swirler blade angle and actuator applied voltage on combustion characteristics and cooling effectiveness." *Fuel* 323 (2022): 124434. https://doi.org/10.1016/j.fuel.2022.124434

[5] Hakim, Kbab, Hamitouche Toufik, and Y. Mouloudj. "Study and simulation of the thrust vectoring in supersonic nozzles." *Journal of Advanced Research in Fluid Mechanics and Thermal Sciences* 93, no. 1 (2022): 13-24. https://doi.org/10.37934/arfmts.93.1.1324

[6] Hosseini, Amirjavad Ahmadian, Maryam Ghodrat, Mohammad Moghiman, and Seyed Hadi Pourhoseini. "Numerical study of inlet air swirl intensity effect of a Methane-Air Diffusion Flame on its combustion characteristics." *Case Studies in Thermal Engineering* 18 (2020): 100610. https://doi.org/10.1016/j.csite.2020.100610

[7] Matthujak, Anirut, Mana Wichangarm, Thanarath Sriveerakul, Sedthawatt Sucharitpwatskul, and Sutthisak Phongthanapanich. "Numerical investigation on the influences of swirling flow to thermal efficiency enhancement of an LPG-energy saving burner." *Case Studies in Thermal Engineering* 28 (2021): 101466. https://doi.org/10.1016/j.csite.2021.101466

[8] Pashchenko, Dmitry. "Hydrogen-rich fuel combustion in a swirling flame: CFD-modeling with experimental verification." *International Journal of Hydrogen Energy* 45, no. 38 (2020): 19996-20003. https://doi.org/10.1016/j.ijhydene.2020.05.113

[9] Ferziger, Joel H., Milovan Perić, and Robert L. Street. *Computational methods for fluid dynamics*. Vol. 3. Berlin: springer, 2002.

[10] Ansys, I. "ANSYS meshing user's guide." *vol* 15317 (2013): 724-746.

[11] Joo, Seongpil, Sanghyeok Kwak, Youngbin Yoon, Sumin Hong, and Daesik Kim. "Experimental and numerical analysis of effect of fuel line length on combustion instability for H2/CH4 gas turbine combustor." *International Journal of Hydrogen Energy* 46, no. 76 (2021): 38119-38131. https://doi.org/10.1016/j.ijhydene.2021.09.031

[12] M., E.A., F.T.M.G.H. M., and I.I. ."Effect of Combustor Diameter on Natural Gas Combustion Characteristic" in Global Journal of ENgineering Science and Research Management 2, no.12 (2015): 9-21.
[13] Mafra, Marcos R., Fábio Luis Fassani, Everton F. Zanoelo, and Waldir A. Bizzo. "Influence of swirl number and fuel equivalence ratio on NO emission in an experimental LPG-fired chamber." *Applied Thermal Engineering* 30, no. 8-9 (2010): 928-934. https://doi.org/10.1016/j.applthermaleng.2010.01.004
[14] Ibrahim, I. A., A. M. Elzallat, M. M. Elsakka, T. M. Farag, and H. M. Gad. "Numerical study of kerosene spray and combustion characteristics using an air-blast atomizer." *Energy Reports* 8 (2022): 5974-5986. https://doi.org/10.1016/j.egyr.2022.04.046
[15] Enagi, Ibrahim I., K. A. Al-Attab, and Z. A. Zainal. "Combustion chamber design and performance for micro gas turbine application." *Fuel processing technology* 166 (2017): 258-268. https://doi.org/10.1016/j.fuproc.2017.05.037
[16] Dixit, Shivanshu, Arvind Kumar, Suraj Kumar, Nitin Waghmare, Harish C. Thakur, and Sabah Khan. "CFD analysis of biodiesel blends and combustion using Ansys Fluent." *Materials Today: Proceedings* 26 (2020): 665-670. https://doi.org/10.1016/j.matpr.2019.12.362
[17] Erkuş, Barış, M. İhsan Karamangil, and Ali Sürmen. "Designing a prototype LPG injection electronic control unit for a carburetted gasoline engine." *Uludağ Üniversitesi Mühendislik Fakültesi Dergisi* 20, no. 2 (2015): 141-153. https://doi.org/10.17482/uujfe.33667
[18] Li, Xinzhuo, Minsung Choi, Chanho Jung, Yeseul Park, and Gyungmin Choi. "Effects of the staging position and air–LPG mixing ratio on the combustion and emission characteristics of coal and gas co-firing." *Energy* 254 (2022): 124314. https://doi.org/10.1016/j.energy.2022.124314
[19] Patel, Vipul, and Rupesh Shah. "Experimental investigation on flame appearance and emission characteristics of LPG inverse diffusion flame with swirl." *Applied Thermal Engineering* 137 (2018): 377-385. https://doi.org/10.1016/j.applthermaleng.2018.03.105
[20] Gherman, Bogdan, Ion Mălăel, Florin Florean, and Ionuţ Porumbel. "Experimental combustion chamber simulation at transient regimes." In *E3S Web of Conferences*, vol. 85, p. 02006. EDP Sciences, 2019. https://doi.org/10.1051/e3sconf/20198502006